31st Annual International Conference of the IEEE EMBS
Minneapolis, Minnesota, USA, September 2-6, 2009

Visual Gate for Brain-Computer Interfaces

N. S. Dias, *Student Member, IEEE,* L. R. Jacinto, *Student Member, IEEE*, P. M. Mendes, *Member, IEEE*, and J. H. Correia, *Member, IEEE*

***Abstract*—Brain-Computer Interfaces (BCI) based on event related potentials (ERP) have been successfully developed for applications like virtual spellers and navigation systems. This study tests the use of visual stimuli unbalanced in the subject's field of view to simultaneously cue mental imagery tasks (left vs. right hand movement) and detect subject attention. The responses to unbalanced cues were compared with the responses to balanced cues in terms of classification accuracy. Subject specific ERP spatial filters were calculated for optimal group separation. The unbalanced cues appear to enhance early ERPs related to cue visuospatial processing that improved the classification accuracy (as low as 6%) of ERPs in response to left vs. right cues soon (150-200 ms) after the cue presentation. This work suggests that such visual interface may be of interest in BCI applications as a gate mechanism for attention estimation and validation of control decisions.**

I. Introduction

Brain-Computer Interfaces (BCI) transform brain signals into control signals [1]. A non-invasive BCI typically uses electroencephalogram (EEG) signals recorded via electrodes placed on the scalp. Some implementations of this interface rely on the detection of sensory-motor rhythms in response to movement imagery tasks in order to control a cursor on the screen [2]. Event related potentials (ERP) in response to mental tasks or attention shift events may be alternatively used to write words on a virtual speller [3]. Besides movement imagery detection accuracy, the identification of an idle or rest state has been of great concern in BCI research [4]. The identification of an idle state may prevent the BCI system from performing undesired actions when the subject is not concerned with movement imagery. Previous studies have detected an idle brain state (i.e. no command) in addition to movement imagery brain responses [4], [5]. In this study, we suggest a virtual implementation of idle state detection by estimating subject attention through visually evoked potentials (i.e. VEP). The spatial arrangement of visual stimuli on a screen affects VEP amplitudes and latencies [6]. Additionally, shifting visual attention between different regions on a screen elicits visual evoked potentials that may be interpreted as indexes of visual spatial selective attention [7]. The possibility of utilizing specific visual interfaces to enhance such VEPs has been used to estimate drivers' attention [8] and select buttons on a screen [9]. The estimation of subject attention (i.e. idle vs. active state) during BCI operation may be used to validate subject control decisions.

This study proposes the use of movement imagery cues (i.e. arrows) commonly used in calibration sessions to simultaneously cue the subject on required movement imagery and estimate subject attention. While arrows centered in the subject's visual field cued the subjects in a first experiment, center-out asymmetric arrows were employed in a second experiment. Event-related potentials (either visually evoked or movement-related) in response to left vs. right cues were classified. The results for both experiment conditions were compared. Spatial filters that enhanced the discrimination of cue-evoked responses were optimized for each subject.

II. Methods

A. Paradigms

Five healthy human subjects, three male and two female, ages 20 to 30, participated in the study. Two different experiments were run, each presenting a paradigm where arrows indicated the imagination tasks to be performed (left vs. right arm movement imaginations).

The subjects were seated approximately 60 cm from a computer screen. The timeline of the trials was the same for all experiments and is illustrated on Fig. 1. Each trial started with a fixation cross, which remained on screen for the entire trial period, at the center of which the subjects were instructed to focus their gaze and attention. An arrow indicating the direction of the imagination task appeared 3 seconds after the cross was made visible. The arrow remained on screen for 4 seconds, i.e. for the duration of the imagination period which started at the appearance of the arrow. Then, both the cross and the arrow disappeared, leaving a blank screen. The length of the inter-trial period was randomly set between 3 and 4.5 seconds to avoid subject adaptation.

Manuscript received April 23, 2009. N. S. Dias is supported by the Portuguese Foundation for Science and Technology (FCT) under grant SFRH/BD/21529/2005. L. R. Jacinto is supported by FCT under grant SFRH/BD/40459/2007.

N. S. Dias, L. R. Jacinto, P. M. Mendes and J. H. Correia are with the Department of Industrial Electronics, University of Minho, Campus Azurem, 4800-058 Guimaraes, Portugal (phone: +351-253-4703; e-mails: ndias@dei.uminho.pt;ljacinto@dei.uminho.pt; paulo.mendes@dei.uminho.pt; higino.correia@dei.uminho.pt).

978-1-4244-3296-7/09/$25.00 ©2009 IEEE

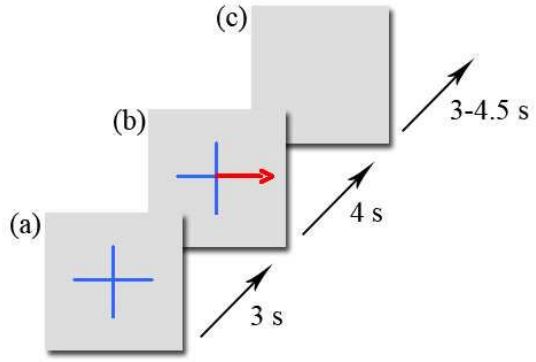

Fig. 1. Example of trial structure and timeline with unbalanced arrows (Experiment 2): (a) start of trial with fixation cross (on screen for 3 s); (b) imagination period with example of arrow cue overlaid on cross (on screen for 4 s); (c) inter-trial period with blank screen (random period of 3 to 4.5 s).

The paradigms differed in arrow type and its position in the subject's visual field. Fig. 2 illustrates examples of the visual cues for each of the two paradigms. In Experiment 1 (Fig. 2a) the arrows appeared centered on a fixation cross (balanced in the subject's visual field), where both ends of the arrow were equidistant from the cross's origin and had both a head and a tail. In Experiment 2 (Fig. 2b) the arrows appeared in a non-centered fashion (unbalanced in the subject visual field) with the total length of each arrow appearing on just one side of the cross's origin and having only a head, but no tail.

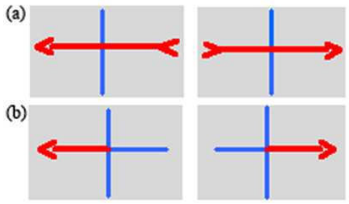

Fig. 2. Visual cues employed for right and left movement imageries at 3 s after trial start for: (a) Experiment 1 with balanced arrows (sessions 1 and 2); (b) Experiment 2 with unbalanced arrows (sessions 3 and 4).

Two sessions of Experiment 1 and two sessions of Experiment 2 were conducted in a total of 4 sessions per subject. Each session consisted of 2 experimental runs of 40 trials with an equal number of each type of cue being presented (i.e. 20 left arrows and 20 right arrows).

B. Recording and Pre-processing

EEG signals were recorded from 19 electrodes (FP1, FP2, F7, F3, Fz, F4, F8, T7, C3, Cz, C4, T8, Pz, P3, Pz, P4, P8, O1 and O2), according to the 10-20 system, all referenced to the linked earlobes. Data were sampled at 256 Hz and band-pass filtered between 0.5 and 60 Hz with a fourth order zero phase Butterworth filter. An ocular artifact removal algorithm was applied to the data [10] to eliminate eye movement related artifacts. Scalp current density (SCD) was estimated from raw filtered EEG data to enhance activity due to superficial cortical sources and minimize activity from deeper sources [11]. SCD was estimated for each electrode location by multiplying the laplacian transformed scalp potentials by the negative of the scalp tissue conductivity as in (1).

$$SCD = -1\Delta L \tag{1}$$

Δ is the scalp conductivity and L is the laplacian transform of the scalp potential. The peripheral frontal and temporal electrodes (i.e. FP1, FP2, F7, F8, T7 and T8) were also excluded from subsequent analyses to further reduce remaining eye movement artifacts that could misguide the calculation of the spatial filters and classification.

C. Epoch Extraction

Data were first low-pass filtered to 8 Hz. Trials (500 ms pre-stimulus to 600 ms post-stimulus) with gradients larger than 40 µV between 2 consecutive time points, absolute amplitudes larger than 50 µV or maximum-minimum amplitude differences of 80 µV were considered artifacts and flagged for removal. The epochs were extracted from a window starting 200 ms before the stimulus up to 600 ms after the stimulus. The mean value of the pre-stimulus period was then subtracted from the post-stimulus activity for baseline correction. To reduce the computational complexity the data were finally downsampled to 20 samples per second. Each final epoch thus contained 12 points representing the 0-600 ms post-stimulus activity. All epochs previously flagged for artifacts were excluded from further processing and analysis.

D. Spatial Filtering and Classification

With the purpose of determining the EEG electrodes that best represent the ERPs in response to stimuli on a subject basis, spatial filters suitable for ERP discrimination were optimized for each subject according to the discriminative spatial patterns approach proposed in [12]. For n electrodes available, the spatial filters $\mathbf{f}$ (n-rows column vector) can be optimally determined from the training data by maximizing criterion J in (2) which can be interpreted as a measure of separation between two groups of feature vectors. Each group represents the EEG epochs recorded in response to either left or right cues. $\mathbf{S_B}$ (n×n matrix) and $\mathbf{S_W}$ (n×n matrix) represent the between and within group scatter matrices respectively.

$$J(\mathbf{f}) = \frac{\mathbf{f}^t \mathbf{S_B} \mathbf{f}}{\mathbf{f}^t \mathbf{S_W} \mathbf{f}} \tag{2}$$

The eigenvectors, as columns of $\mathbf{V}$ (n×n matrix) and the eigenvalues are the solution of the generalized eigenvalue problem $\mathbf{S_B}$ / $\mathbf{S_W}$ where the eigenvectors may be used as spatial filters and the eigenvalues represent the discriminative power of the filters.

Table I. Minimal Classification error (%) results and respective latencies (ms) evaluated in an early period (50-250 ms) and in a late period (300-600 ms) for 5 subjects for all 4 sessions.

Exp. (session)	Subject A				Subject B				Subject C				Subject D				Subject E			
	Early		Late		Early		Late		Early		Late		Early		Late		Early		Late	
	Err. (%)	Lat. (ms)	Err. (%)	Lat. (ms)	Err. (%)	Lat. (ms)	Err. (%)	Lat. (ms)	Err. (%)	Lat. (ms)	Err. (%)	Lat. (ms)	Err. (%)	Lat. (ms)	Err. (%)	Lat. (ms)	Err. (%)	Lat. (ms)	Err. (%)	Lat. (ms)
1 (1)	32	200	**29**	600	27	200	27	350	26	250	**15**	600	28	100	**21**	400	31	150	**26**	300
1 (2)	27	200	27	350	**21**	50	22	400	22	250	**10**	550	22	250	**15**	600	28	50	**25**	550
2 (3)	**16**	200	27	600	**19**	200	26	550	10	200	**9**	300	21	100	**12**	450	**17**	200	21	300
2 (4)	**8**	200	28	350	**16**	200	24	400	-	-	**6**	450	**22**	150	23	450	**18**	200	22	450

The new feature vectors, as columns of $\mathbf{Y}_i$ ($n \times m$ matrix: for m epoch sample points), result from the spatial filtering of the data epochs $\mathbf{X}_i$ ($n \times m$ matrix) by the determined filters as calculated in (3). The subscript i indicates the epoch.

$$\mathbf{Y}_i = \mathbf{V}^t \mathbf{X}_i + \mathbf{V}_0 \tag{3}$$

The unidimensional projections (rows of $\mathbf{Y}_i$) are unbiased by the term $\mathbf{V_0} = -\mathbf{V}^t\mathbf{M}$ where $\mathbf{M}$ represents the average of $\mathbf{X}_i$ across all epochs i. The calculated projections may be considered as virtual channels that optimize group discrimination by minimizing the variance of the data along the projection while maximizing the difference between the projected group means. A form of Fisher Discriminant Analysis was applied to discriminate the projected samples in $\mathbf{Y}$ and predict group membership according to (4).

$$\mathbf{Z} = \mathbf{Y}^t \mathbf{b} \tag{4}$$

The coefficients $\mathbf{b}$ (n-rows column vector) were calculated as in [13] since this approach appears to deal better with EEG data dynamics than regular Fisher's approach. Discrimination quality was assessed through the mean prediction error rate calculated over 10 repetitions of a 10-fold cross-validation scheme. The spatial filters were calculated for the training data (90%) of each session and their accuracy was tested on the validation data (10%) from the same session.

III. Results

Table I presents the classification results of 100 cross-validation folds for each subject. In each session, the minimum classification error was evaluated in two distinct periods: an early period from 50 ms to 250 ms after cue presentation; and a later period from 300 ms to 600 ms after cue presentation. The classification errors for the paradigm with balanced arrows (Experiment 1) were between 21% and 32% in the early period and between 10% and 29% in the later period.

The classification errors for the paradigm with unbalanced arrows (Experiment 2) were between 8% and 22% in the early period and between 6% and 28% in the later period. The classification errors were generally lower when unbalanced arrows were employed, especially for the earlier period. Exceptionally, the results for Subject C did not present any visible minimum for the early period in session 4.

Fig. 3 illustrates the averaged classification results over time for subject E. The error minima for both periods can be observed in all sessions. The unbalanced arrows sessions (sessions 3 and 4) show lower mean classification errors for both the early and the later period, except for the later period of session 3, when compared with the mean errors for the balanced arrows (sessions 1 and 2).

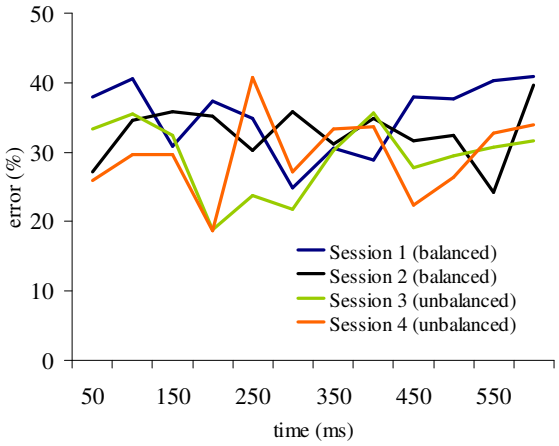

Fig. 3. Average classification error rate for subject E for the balanced arrows paradigm (Experiment 1), sessions 1 and 2, and for the unbalanced arrows paradigm (Experiment 2), sessions 3 and 4.

Fig. 4 shows the topographical maps of two spatial filters calculated for sessions 1 (balanced arrows) and 3 (unbalanced arrows) of subject A. Figure 4a refers to session 1 and shows increased filter weights for frontal and central electrodes. In contrast, Figure 4b shows highest weights on parietal and occipital electrodes for session 3. These results generalized well for other subjects.

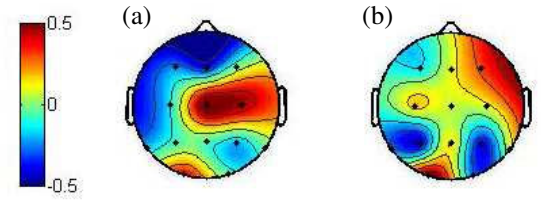

Fig. 4. Topographical maps of two spatial filters calculated from scalp current densities of subject A. The electrode weights are presented for (a) session 1 (balanced arrows paradigm) and (b) session 3 (unbalanced arrows paradigm).

IV. Discussion and Conclusions

This work studied the effect of commonly used movement imagery cues (either balanced or unbalanced in subjects' visual field) on the amplitude and latencies of cue-evoked responses. The observed classifications errors for left vs. right arrows suggest that the unbalanced cues are capable of eliciting enlarged lateralized responses as soon as 150-200 ms after cue presentation. Additionally, for some subjects, an increase of the classification accuracy in a later period (300-600 ms) was also observed. The spatial distribution of the filters calculated for sessions presenting unbalanced cues show predominant activation of vision-related brain regions, suggesting that the early error minima are due to VEPs that reflect visuospatial processing differences between left and right cues. In opposition, the spatial distribution of the filters for the balanced arrow cues suggests the activation of motor-related brain regions. It is noted that the spatial distribution of the filters for the sessions employing balanced cues also shows slight activation of the occipital region despite the predominance of the central region. This fact points to remaining differences on the visuospatial processing required by left vs. right balanced cues.

The presented results suggest that the display of unbalanced arrows is responsible for triggering enhanced visual evoked brain responses, as early as 150-200 ms. Previous studies have shown that non-centered cues tend to generate early visual ERPs with enlarged amplitudes as a result of attention allocation in visual space [7]. Similarly, the visuospatial attention mechanism may have enhanced the discrimination of left vs. right cues during the early time period. Therefore, arrows unbalanced in the subject's field of view may be displayed in order to improve the detection of "idle" vs. "active" states of the subject thus validating later decisions based on movement imagery detection or other mental tasks. From our results, it remains unclear what is the correlation between the observed early (150-200 ms) error minima and the later (300-600 ms) error minima. Our future work will address this issue. Nevertheless, our findings suggest that such visual interfaces may be used as a gate mechanism in BCI systems for overall improvement of BCI performance.

References

[1] G. Pfurtscheller and G. Neuper C, "Motor imagery and direct brain-computer communication," *IEEE Proc*, vol. 89, no. 7, pp. 1123-1134, Jul. 1981.

[2] J. R. Wolpaw, D. J. McFarland and T. M. Vaughan, "Brain–Computer Interface Research at the Wadsworth Center," *IEEE Trans Rehabil Eng*, vol.8, no 2, pp. 222-226, Jun. 2000.

[3] F. Nijboer *et al.*, "A P300 based brain-computer interface for people with amyotrophic lateral sclerosis," *Clin Neurophysiol*, Vol 119, no 8, pp. 1909-1916, Aug. 2008.

[4] D. Zhang, Y.Wang, X. Gao, B. Hong, and S. Gao (2007, July). "An algorithm for idle-state detection in motor-imagery-based brain-computer interface". *Comput Intell Neurosci* [online]. Vol 2007. Available: http://www.hindawi.com/journals/cin/

[5] A. Bashashati, R. K. Ward and G. E. Birch (2007, July). "Towards development of a 3-state self-paced brain-computer interface". *Comput Intell Neurosci* [online]. Vol. 2007. Available: http://www.hindawi.com/journals/cin/

[6] S. Yamaguchi, H. Tsuchiya and S. Kobayashi, "Electroencephalographic activity associated with shifts of visuospatial attention," *Brain*, vol. 117, pt. 3, pp. 553-562, June 1994.

[7] M. M. Müller and S. Hillyard, "Concurrent recording of steady-state and transient event-related potentials as indices of visual-spatial selective attention," *Clin Neurophysiol*, vol. 111, no 9, pp. 1544-52, Sep. 2000.

[8] B. S. Reddy, O. A. Basir and S. J. Leat, "Estimation of driver attention using visually evoked potentials (Published Conference Proceedings Style)," in *Proc IEEE Intelligent Vehicles Symposium*, Istanbul, 2007, pp. 588-593.

[9] F. Guo, B. Hong, X. Gao and S. Gao, "A brain-computer interface using motion-onset visual evoked potentials," *J Neural Eng*, vol. 5, no 4, pp. 477-485, Dec. 2008.

[10] G. Gratton, M. G. H. Coles and E. Donchin E, "A new method for the off-line removal of ocular artifact," *Electroencephalogr Clin Neurophysiol*, vol. 55, no 4, pp. 468-84, Apr. 1983.

[11] F. Perrin, J. Pernier, O. Bertrand and J. F. Echallier, "Spherical splines for scalp potential and current density mapping," *Electroencephalogr Clin Neurophysiol*, vol. 72, no 2, pp. 184-187, Feb 1989 (Corrigenda EEG 02274, *Electroencephalogr Clin Neurophysiol*, vol. 76: 565, 1990).

[12] X. Liao, D. Yao, D. Wu and C. Li, "Combining spatial filters for the classification of single-trial EEG in a finger movement task," *IEEE Trans Biomed Eng*, vol. 54, no 5, pp. 821-831, May 2007.

[13] S. J. Schiff, T. Sauer, R. Kumar and S. K. Weinstein, "Neuronal spatiotemporal pattern discrimination: The dynamical evolution of seizures," *Neuroimage*, vol. 28, no 4, pp. 1043-1055, Dec. 2005.